HHS Public Access

Author manuscript

J Invest Dermatol. Author manuscript; available in PMC 2024 June 01.

Published in final edited form as:

J Invest Dermatol. 2023 June ; 143(6): 1052–1061.e3. doi:10.1016/j.jid.2022.12.009.

Involucrin modulates vitamin D receptor activity in the epidermis

Alina D. Schmidt[1,2,3], **Charlene Miciano**[1,2,3], **Qi Zheng**[4], **Mary Elizabeth Mathyer**[1,2,3], **Elizabeth A. Grice**[4], **Cristina de Guzman Strong**[1,2,3,5,6,¶]

[1]Division of Dermatology, Department of Medicine, Washington University in St. Louis School of Medicine, St. Louis, MO, 63110 USA

[2]Center for Pharmacogenomics, Department of Medicine, Washington University in St. Louis School of Medicine, St. Louis, MO, 63110 USA

[3]Center for the Study of Itch & Sensory Disorders, Washington University in St. Louis School of Medicine, St. Louis, MO 63110 USA

[4]Department of Dermatology, University of Pennsylvania Perelman School of Medicine, Philadelphia, PA 19104 USA

[5]Center for Cutaneous Biology and Immunology, Department of Dermatology, Immunology Program, Henry Ford Cancer Institute, Henry Ford Health, Detroit, MI 48202 USA

[6]Department of Medicine, College of Human Medicine, Michigan State University, East Lansing, MI 48824

Abstract

Terminally differentiated keratinocytes are critical for epidermal function and surrounded by involucrin (IVL). Increased *IVL* expression is associated with a near selective sweep in European populations compared to African. This positive selection for increased *IVL* in the epidermis identifies human adaptation out-of-Africa. The functional significance is unclear. We hypothesize Ivl to modulate the environmentally sensitive Vitamin D receptor (Vdr) in the epidermis. We investigated Vdr activity in *Ivl* −/− and wild-type (WT) mice using vitamin D agonist (MC903) treatment and comprehensively determined the inflammatory response using single-cell RNA sequencing (scRNA-seq) and associated skin microbiome changes using 16S bacterial phylotyping. Vdr activity and target gene expression were reduced in *Ivl* −/− mouse skin, with decreased MC903-mediated skin inflammation and significant reductions in CD4+ T cells, basophils, macrophages, monocytes, and type II basal keratinocytes and increase in suprabasal

¶ **To Whom Correspondence Should Be Addressed**: **Cristina de Guzman Strong, PhD.**, Center for Cutaneous Biology and Immunology, Department of Dermatology, Immunology Program, Henry Ford Cancer Institute, Henry Ford Health, 1 Ford Place RM 4D46, Detroit, MI 48202 USA, Tel: (313) 876-7291, cstrong4@hfhs.org, Twitter: @cdgstrong21.

AUTHOR CONTRIBUTIONS

Conceptualization: CdGS; Data Curation: ADS, CM, QZ, CdGS; Formal Analysis: ADS, CM, QZ, EAG, CdGS; Funding Acquisition: EAG, CdGS; Investigation: ADS, CM, QZ, MEM, EAG, CdGS; Methodology: ADS, CM, QZ, MEM, EAG, CdGS; Project Administration: EAG, CdGS; Resources: EAG, CdGS; Software: ADS, CM, QZ; Supervision: EAG, CdGS; Validation: ADS, CdGS; Visualization: ADS, CM, QZ, CdGS; Writing – Original Draft Preparation: ADS, MEM, CdGS; Writing – Review and Editing – ADS, CM, QZ, MEM, EAG, CdGS.

keratinocytes. Coinciding with the dampened MC903-mediated inflammation, skin microbiota of *Ivl* −/− mice was more stable compared to WT mice, which exhibited a MC903-responsive increase in Bacteroidetes and decrease in Firmicutes. Together, our studies in *Ivl* −/− mice identify a functional role for Involucrin to positively impact Vdr activity and suggest an emerging IVL/VDR paradigm for adaptation in the human epidermis.

INTRODUCTION

The epidermis is the outermost tissue of the skin, providing crucial barrier function against the external environment (Watt, 2014, Matsui and Amagai, 2015). It is composed of a hierarchical structure of proliferating and differentiated epidermal cells or keratinocytes that form the essential “brick” units of the skin barrier. The epidermis is also the primary site of vitamin D3 production (Bikle and Christakos, 2020). Keratinocytes are also known to elicit proper recruitment of immune cells in response to breaks in the skin barrier, a key defense mechanism to maintain skin homeostasis (Niec et al., 2021). Keratinocytes as well respond to microbiota exposure with the induction of key epidermal differentiation gene expression (Meisel et al., 2018) (Uberoi et al., 2021). Indeed, the biology of epidermal keratinocytes is complex and challenging and coupled with the need for these cells to quickly adapt amidst differing environments in order to ensure survival.

Differentiated keratinocytes express many genes encoded within the Epidermal Differentiation Locus (EDC) critical for barrier function (Volz et al., 1993, Mischke et al., 1996, Zhao and Elder, 1997, de Guzman Strong et al., 2010). One important EDC gene is involucrin (IVL), whose expression is a major marker for early epidermal differentiation (Rice and Green, 1979). IVL is a scaffolder for many cross-linked proteins that together form the mature cornified envelope (CE) surrounding the terminally differentiated keratinocyte (Eckert and Green, 1986, Steinert and Marekov, 1995, Robinson et al., 1996, Nemes et al., 1999, Kajava, 2000). Given the importance of CE formation for barrier function, it was surprising to find that *Ivl* knockout (−/−) mice exhibited no defects in the epidermal barrier and cornified envelope formation (Djian et al., 2000). However, triple knockout mice for *Ivl*, *envoplakin* (*Envl*), and *periplakin* (*Ppl*) cornified envelope genes exhibited a delay in developmental barrier formation, dry, flaky skin, and persistent hyperkeratosis (Sevilla et al., 2007). Together, these studies revealed that Ivl alone is dispensable for skin barrier development but, with coinciding Envl and Ppl deficiencies, is critical for epidermal barrier function.

We recently discovered positive selection for a human *IVL* allele in populations of European ancestry (Mathyer et al., 2021). We identified a specific *IVL* haplotype that underwent a near selective sweep (>95% allele frequency [AF]) in contrast to that in Africa (32% AF). The European *IVL* haplotype consists of expression quantitative trait loci (eQTLs) associated with increased *IVL* gene expression in the skin in contrast to relatively lower *IVL* expression in the skin of African ancestry. To our knowledge, this is the first report of recent evolutionary adaptation in the human epidermis. Our finding suggests a selective benefit for increased *IVL* as humans migrated out of Africa. Here we revisit the role of involucrin for adaptation in the epidermis in response to the environment.

The vitamin D receptor (Vdr) was recently determined to exhibit environmental sensitivity (Romney et al., 2018). This was discovered in killifish that exhibited differential downstream Vdr signaling when grown under different temperature conditions. Motivated by this novel discovery for Vdr as an environmentally sensitive receptor and its known expression in epidermal keratinocytes (Stumpf et al., 1979), we reasoned VDR as a potential molecule that could link the levels of involucrin in the skin to environmental sensitivity and hence relevant to human epidermal adaptation. VDR is known to stimulate epidermal differentiation when activated by the vitamin D metabolite, 1,25-$(OH)_2$D, produced by keratinocytes (Hosomi et al., 1983, Bikle, 2011). Knockout mouse studies confirmed a requirement for Vdr for epidermal differentiation as Vdr null mice exhibited reduced levels of involucrin, filaggrin, and loricrin (Xie et al., 2002, Bikle et al., 2006), resulting in a defective permeability barrier (Oda et al., 2009) and immune response (Schauber et al., 2007, Muehleisen et al., 2012). Interestingly, VDR and vitamin D3 levels decrease upon IVL-marked terminal differentiation, suggesting IVL-associated negative feedback regulation for VDR (Horiuchi et al., 1985, Pillai et al., 1988). Moreover, VDR nuclear localization was found to be significantly reduced in the epidermis of black donor normal skin compared to that of white donors (Hahn and Supp, 2017) whose genotypes we have determined to be more commonly associated with relatively increased *IVL* (Mathyer et al., 2021). The findings using knockout mice and in vitro studies highlight a putative relationship between IVL and VDR. The more recent study using human diverse skin further suggests a role for higher IVL levels and its potential direct, downstream dosage effect on VDR to modulate epidermal function and underlie population-specific, human skin adaptation.

We hypothesized a role for involucrin to modulate Vdr activity as a mode by which the epidermis adapts to the environment. To test this hypothesis, we investigated Vdr function in the epidermis of *Ivl* −/− mice with vitamin D agonist (MC903) exposure and determined the impact using single-cell RNA sequencing (scRNA-seq), flow cytometry, and 16S rRNA bacterial phylotyping to assess Vdr activated-skin inflammation and the anticipated, associated changes to the skin microbiome. Here we report decreased Vdr activity and Vitamin D-responsive gene expressions in *Ivl* −/− mice that exhibited reduced MC903-induced inflammation marked by scRNA-seq identification for decreased basophils, macrophages, monocytes, and $CD4^+$ T cells and subsequent validation for decreased $CD11b^+$ IgE^+ basophils and CD4+ T cells and newly discovered increase in $CD11b^+$ IgE^{high} mast cells by flow cytometry. The decrease in Vdr-mediated inflammation in *Ivl* −/− mice coincided with no phylum level changes to the skin microbiome in contrast to WT that exhibited an MC903-responsive dysbiosis with increase in Bacteroidetes and decrease in Firmicutes. Together, our findings identify a functional role for Ivl to positively impact Vdr activity for the skin immune response in the epidermis.

RESULTS

Vdr-mediated inflammation is reduced in MC903-treated *Ivl* −/− mouse skin

We investigated Vdr function in *Ivl* −/− and wild-type (WT) mice by way of MC903-mediated activation. *Ivl* −/− and WT mouse ear skin were treated daily for 12 days with

MC903 that results in skin inflammation (Li et al., 2006, Kim et al., 2013, Moosbrugger-Martinz et al., 2017, Walsh et al., 2019). MC903-treated WT mice exhibited ear thickening and scaling compared to ethanol-treated ears (Figure 1a). By contrast, MC903-treated *Ivl* −/− mice exhibited less ear thickening and scaling. Histological findings further identified epidermal hyperplasia and hyperkeratosis observed in MC903-treated WT ear skin that was strikingly less evident in MC903-treated *Ivl* −/− and absent in ethanol-treated ear skin (Figure 1b). We assessed the longitudinal development of ear thickness over the 12-day treatment period and found an overall trend for decreased MC903-induced skin inflammation in *Ivl* −/− mice compared to WT (Figure 1c, Figure S1). Decreased inflammation in *Ivl* −/− mice was significant on days 6 and 7 and for each of days 9–12 (day 6, $p = 0.044$; day 7, $p = 0.016$; day 9, $p = 0.039$; day 10, $p = 0.016$; day 11, $p = 0.007$; and day 12, $p = 0.004$; one-way ANOVA with post-hoc Tukey HSD). Together, our findings for decreased skin inflammation in MC903-treated *Ivl*–/− adult mice identifies decreased Vdr activity in *Ivl* −/− epidermis.

scRNA-seq identifies a decrease in Vitamin D-responsive gene expressions and decreased basophils, CD4$^+$ T cells, macrophages, monocytes, and basal II keratinocytes and increased suprabasal keratinocytes in MC903-treated *Ivl* −/− skin

We next determined the cell types that underlie the Vdr-mediated inflammatory response at a single-cell resolution using scRNA-seq. Single-cell suspensions from MC903-treated ear skin from *Ivl* −/− and WT mice were obtained for scRNA-seq (10X Genomics). A total of 25,799 single cells were sequenced and analyzed from both *Ivl* −/− and WT mice (n=2 for each genotype). Seurat4.0 clustering analyses identified 20 cell populations in MC903-treated ear skin (Figure 2a). Keratinocytes comprise a majority of the populations with 13 distinct keratinocyte clusters that were identified in both genotypes (Figure 2b). Additionally, five immune cell types were found including basophils, macrophages, monocytes, natural killer T cells, and CD4$^+$ T cells, with the remaining two populations comprised of fibroblasts and melanocytes. We confirmed annotation of the cell clusters using gene markers specific for each cell population (Joost et al., 2016) (Tables S1-2).

We next investigated the impact of MC903 treatment on Vitamin D-responsive gene expression in *Ivl* −/− mice that exhibited a dampened Vdr-mediated inflammatory response. Fourteen Vdr-regulated genes in GSEA (GOBP_RESPONSE_TO_VITAMIN_D; MM6812) were expressed in at least one scRNA-seq cell cluster for either MC903-treated *Ivl* −/− or WT skin (Figure 2c, Figure S2). Of these, ten genes were differentially expressed in at least one scRNA-seq cell cluster in MC903-treated *Ivl* −/− vs. WT skin (adj $p < 0.05$; Table S3). A majority of these gene expression differences in *Ivl* −/− skin were decreased (38 out of 41 clusters) and were found primarily in the keratinocyte clusters (17 out of 38 decreased clusters). *Vdr*, *Cyp24a1*, *Snw1*, *Pdia3*, and *Rxra* were the top 5 differentially expressed genes that were observed in at least 3 clusters (Figure 2c). *Vdr*, *Snw1*, and *Pdia3* were all decreased in basal cycling (0), suprabasal cycling (3), and suprabasal infundibular (6) keratinocytes in MC903-treated *Ivl* −/− mice. More importantly, *Vdr* was the top gene that was found to have the most number of keratinocyte clusters exhibiting differential expression, a total of 9 that were all decreased in *Ivl* −/− mice. By contrast, Vdr-regulated *Cyp24a1* was increased in several *Ivl* −/− keratinocyte clusters and melanocytes. *Cyp24a1*

encodes 24-hydroxylase that breaks down active Vitamin D (Makin et al., 1989, Reddy and Tserng, 1989, Schlingmann et al., 2011). The finding for increased *Cyp24a1* in MC903-treated *Ivl* −/− skin suggests a compensatory mechanism in response to MC903 and likely non-Vdr regulated given the decreased *Vdr* expression in these mice. Together, our findings identifies significant decreases in Vdr and Vitamin D-responsive genes that underlie the dampened MC903-mediated inflammation in *Ivl* −/− mice.

We further determined if there was a difference in the proportions between each scRNA-seq population in MC903-treated *Ivl* −/− mice compared to WT. The proportions for each of five cell populations were significantly reduced in MC903-treated *Ivl* −/− mice: basophils, macrophages, basal IIb keratinocytes, $CD4^+$ T cells, and monocytes (Figure 2d, chi-squared goodness of fit, $p < 0.00001$, $p < 0.00001$, $p < 0.00001$, $p < 0.0455$, and $p < 0.00014$, respectively). However, suprabasal keratinocytes were significantly increased in MC903-treated *Ivl*−/− ear skin (Figure 2d, chi-squared goodness of fit, $p < 0.028$) and concomitant with a decrease in basal IIb keratinocytes. The finding suggests a higher turnover in basal IIb keratinocytes and downstream effect for the increased number of suprabasal keratinocytes. The reduction in basophils led us to further investigate the significance of IL-4 and IL-6 that are also known key drivers for MC903-induced skin inflammation (Kim et al., 2014, Hussain et al., 2018, Walsh et al., 2019). Our scRNA-seq analysis resolved predominant IL-4 and IL-6 expressions in basophils as shown in MC903-treated mice and for which basophil numbers were significantly decreased in the *Ivl* −/− mice (Figure 2de). In summary, scRNA-seq resolves the single cell architecture of the dampened MC903-induced inflammation in *Ivl* −/− mice identifying reduced basophils, macrophages, $CD4^+$ T cells, monocytes, and a notable keratinocyte response (basal IIb keratinocyte depletion with increased suprabasal cells) and further highlights skin immune cellular interconnectivity.

Flow cytometry validates decreased CD4+ T cells and basophils and reveals increased mast cells in MC903-treated *Ivl* −/− mouse skin

We sought to validate the scRNA-seq-identified immune cell types that were reduced in MC903-treated *Ivl* −/− compared to WT mice by flow cytometry. $CD4^+$ T cells, $CD11c^+$ dermal dendritic cells, granulocytes, monocytes, eosinophils, and $CD8^+$ T cells were previously determined to be increased based on immunofluorescent and histological findings in MC903-induced inflamed skin (Li et al., 2006). However, of the $CD45^+$ leukocytes in the MC903-treated skin, we found no significant differences in dendritic cells ($CD11c^+$), eosinophils ($CD11b^+$, $Ly6g^-$), neutrophils ($CD11b^+$, $Ly6g^+$) and B cells ($CD19^+$) between *Ivl* −/− and WT mice (Figure S3). We also did not find significant differences in monocytes ($CD11b^+$, $F4/80^-$, $Ly6g^-$) and macrophages ($CD11b^+$, $F4/80^+$, $Ly6g^-$) (Figure 3ab). However, both $CD4^+$ T cells and $CD11b^+$ IgE^+ basophils were significantly reduced in *Ivl* −/− compared to WT treated ear skin (Figure 3ab, one-sided *t*-test, $p < 0.04$, $p < 0.05$) respectively. Interestingly, we also observed an increase in a distinct population of $CD11b^+$ IgE^{high} cells in MC903-treated *Ivl* −/− skin, representative of mast cells that was significantly increased compared to MC903-treated WT ear skin (one-sided *t*-test, $p < 0.03$) (Figure 3ab). Together, our flow cytometry results confirm our scRNA-seq findings for decreased basophil and $CD4^+$ T cell infiltrates yet with an additional discovery for increased $CD11b^+$ IgE^{high} mast cells in MC903-treated *Ivl* −/− mice.

MC903-treated WT skin exhibit increased Bacteroidetes and decreased Firmicutes whereas *Ivl −/−* untreated skin exhibit increased Firmicutes (*Streptococcus* and *Aerococcus*) and decreased Bacteroidetes (*Muribaculaceae*) *OTUs*

We next examined the impact of Vdr-mediated inflammation on *Ivl* −/− and WT skin microbiomes. Specific microbiome changes (dysbiosis) are sufficient to drive skin inflammation as observed in barrier-impaired, ADAM17-deficient mice (Kobayashi et al., 2015). However, whether Vdr-mediated inflammation drives microbial changes per se is an underexplored area of investigation. The dampened Vdr activity and decreased *Vdr* and Vitamin D-responsive gene expression in *Ivl* −/− skin also provides us with the opportunity to more directly address the microbial changes specific to Vdr activity that are active in WT and compromised in *Ivl* −/− skin. As microbiota exposure induces host expression of involucrin in the skin (Meisel et al., 2018, Uberoi et al., 2021), we further explore the significance of involucrin for shaping microbial community structure.

To profile skin microbiota dynamics, we used 16S rRNA sequencing of the V1-V3 hypervariable region to identify bacterial taxa from ear swab collections from 12-week-old mice before and after MC903 treatment. 16S microbiome sequencing reads were individually phylotyped and subsequently clustered into phylogeny-based operational taxonomic units (OTUs) (Zheng et al., 2018). We first assessed the beta (inter-sample) diversity with respect to MC903 treatment in *Ivl* −/− and WT skin and observed that clustering between microbial communities was significantly associated with both genotypes (WT or *Ivl* −/−) and MC903 treatment (before or after) (Figure 4a, $p < 0.005$, PERMANOVA test) (GreenGenes v13.8 (DeSantis et al., 2006)). Closer examination of the microbial phyla on untreated WT skin revealed a composition dominated by the phylum Firmicutes and phylum Bacteroidetes consistent with previous reports in WT murine ear skin microbiota (Ren et al., 2017, Moskovicz et al., 2021) (Figure 4b). By contrast, we found reductions in Bacteroidetes, Actinobacteria, and Verrucomicrobia and an increase in Firmicutes in *Ivl* −/− untreated skin compared to WT (Figure 4b). We next compared the alpha diversity (intra-sample) of untreated WT and *Ivl* −/− skin by calculating the Shannon Index, which takes into account both richness and evenness of operational taxonomic units (OTUs) observed in a sample. We detected a significant depletion in the alpha diversity of untreated *Ivl* −/− skin compared to WT ($p < 0.001$, *t*-test) (Figure 4c).

We next determined the longitudinal effect of MC903 treatment on the skin microbiota. MC903 treatment in WT skin resulted in an increase in phylum Bacteroidetes and a decrease in phylum Firmicutes compared to untreated skin (Figure 4d). In contrast, MC903 treatment in *Ivl* −/− skin did not change the phylum composition of the skin microbiota compared to untreated *Ivl* −/− skin (Figure 4d). Yet alpha diversity in MC903-treated *Ivl* −/− skin was significantly reduced compared to MC903-treated WT skin and correlates with the dampened skin inflammation in *Ivl* −/− treated skin compared to WT treated skin ($p < 0.05$) (Figure 4e). Relative to untreated skin, alpha diversity in WT mice was significantly reduced after MC903 treatment (Figure 4f, $p < 0.05$, *t*-test). In contrast, alpha diversity in *Ivl* −/− mice did not change after MC903 treatment, albeit with a slight increase compared to baseline skin (Figure 4f). Together, our results reveal potential dysbiosis in *Ivl* −/− baseline skin marked by a decrease in Bacteroidetes, Actinobacteria, and Verrucomicrobia and an

increase in Firmicutes phyla. These changes were also consistent with a significant decrease in alpha diversity that persisted even upon MC903 treatment. We further identified dysbiosis in our longitudinal study of WT skin upon MC903 treatment marked by an increase in Bacteroidetes, a decrease in Firmicutes, and a significant reduction in alpha diversity.

We next determined the differentially enriched OTUs (DE-OTUs) that underlie the microbiota differences observed in *Ivl* −/− skin and upon MC903 treatment in WT skin. We compared the abundance of each phylogeny-based OTU per mouse group before and after treatment (Love et al., 2014). In untreated skin, we identified 122 upregulated and 28 downregulated differentially enriched OTUs (DE-OTUs) in *Ivl* −/− skin compared to WT (Figure 4g, Table S4). A majority of the top 15 upregulated OTUs in *Ivl* −/− untreated skin (66%) were comprised of phylum Firmicutes *(Aerococcus, Streptococcus, Lachnospiraceae,* and *Muris)*. By contrast, the most common taxa of the top 15 downregulated OTUs in *Ivl* −/− untreated skin were *Muribaculaceae* (Bacteroidetes phylum) (47%) and formerly known as S24–7 (Ormerod et al., 2016). In MC903-treated skin, we identified a total of 115 upregulated and 52 downregulated DE-OTUs (Figure 4h, Table S5) in *Ivl* −/− skin vs. WT. Similar to untreated skin, a majority (66%) of the top 15 upregulated OTUs in MC903-treated *Ivl* −/− skin were comprised of members from the phylum Firmicutes (*Aerococcus* and *Streptococcus*). Again, similar to untreated skin, a majority (60%) of the downregulated OTUs were Bacteroidetes (*Muribaculaceae*).

In summary, our results suggest changes to the skin microbiota in *Ivl* −/− skin that were stable even after MC903 treatment. Our longitudinal study further identifies alterations to the microbiota in WT and not in *Ivl* −/− skin with decreased Vdr-mediated inflammation. This supports the hypothesis that Vdr-mediated inflammation can drive dysbiosis. As housing conditions can influence the skin microbiota, future studies using isolated cages and additional single-housed mice can further bolster these findings and provide insight into the cause and effect relationship between host and microbiota.

DISCUSSION

Our study identifies a functional role for *Ivl* to positively regulate Vdr activity in the epidermis. Here we find that Vdr activation and several Vitamin D-responsive genes including Vdr are reduced in MC903-treated *Ivl*−/− mice resulting in a dampened Vdr-mediated inflammatory response. The response is characterized by a significant reduction in CD4+ T cells, decreases in basophils, monocytes, macrophages, and basal II keratinocytes, and a concomitant increase in suprabasal keratinocytes. Indeed, MC903 is an analog of the natural VDR ligand, 1,25-$(OH)_2$D, yet its topical application also stimulates VDR activity, resulting in skin inflammation albeit at a lower calcemic activity (Carlberg, 2003). We further validated our scRNA-seq findings for increased CD4+ T cells and basophils in MC903-treated WT skin but also discovered an increase in mast cells in MC903-treated *Ivl* −/− skin. Although flow cytometry did not fully recapitulate the scRNA-seq findings for monocytes and macrophages, not all monocytes and macrophage clusters as determined by scRNA-seq directly correlate with cell surface marker expression (Sanin et al., 2022). Indeed, recent scRNA-seq studies have determined that multiple subsets of monocytes and their derived macrophages exist and each marked by dynamic heterogeneity in its

transcriptional programs (Villani et al., 2017, Zilionis et al., 2019, Sanin et al., 2022). This also creates even more challenges to further resolve these subset(s) and ascribe function. Nevertheless, increased monocytes have been reported in several MC903 studies (Li et al., 2006, Kim et al., 2013, Walsh et al., 2019). Future studies are needed to further resolve the monocyte subsets impacted in the context of MC903-mediated inflammation and other inflammatory conditions. Additionally, *Ivl* −/− skin also exhibited microbial dysbiosis with increases in Firmicutes phyla, *Streptococcus* and *Aerococcus*, and a decrease in Bacteroidetes *Muribaculaceae* that was sustained even after MC903 treatment. Together, our results identify a functional role for involucrin to facilitate Vdr signaling in the epidermis for skin immune crosstalk and cellular composition as well as for impacting the microbial community structure.

Previous work in vitro suggested a potential negative feedback for IVL on VDR (Horiuchi et al., 1985) (Pillai et al., 1988). VDR and Vitamin D3 levels concomitantly decreased and coincided with the onset of IVL-marked terminal differentiation as determined in cultured keratinocytes. However, our in vivo work in mice challenges this notion and rather establishes that the presence of involucrin instead positively regulates epidermal VDR activity. This is further supported by our scRNA-seq findings in *Ivl* −/− keratinocyte clusters for decreased *Vdr* and *Snw1*, *Pdia3*, and *Rxra* that co-regulate with Vdr (Quack and Carlberg, 2000, Zhang et al., 2003, Chen et al., 2013).

The increase in mast cells observed in MC903-treated *Ivl* −/− mice is notable despite the dampened skin inflammation yet observed dysbiosis. Mast cells are long-lived (up to 30 days) in contrast to short-lived basophils (up to 3 days) and hence are likely to reflect a more sustained cellular response to an environmental trigger (Igawa and Di Nardo, 2017). Interestingly, it was recently discovered that germ-free mice have immature mast cells (Wang et al., 2017). Skin microbiota reconstitution in these mice facilitated normal mast cell maturation thus identifying a functional role for microbiota in shaping mast cell differentiation. We speculate, based on these findings, that the observed mast cell increase in MC903-treated *Ivl* −/− mice may likely arise from prior skin dysbiosis and warrants future investigations.

Additionally, our findings for potential dysbiosis in *Ivl*-deficient mouse skin suggests a requirement for involucrin to maintain microbial homeostasis in comparison to its reference WT isogenic C57Bl/6 mouse strain. We further identify dysbiosis associated with Vdr-mediated inflammation in WT skin. Indeed, additional studies are needed to more completely exclude the possibility of cage effects in comparing Ivl-deficient to WT skin microbiota at baseline yet we included the collection and analysis of negative and positive control specimens to minimize this concern. With our longitudinal study design, we were able to capture the changes in the microbiome due to treatment. Even with the observed microbiota changes, the microbiome of *Ivl*−/− skin does not appear to give rise to pathogenic infection even after MC903 treatment and also over time as we did not observe any overt infections in MC903-treated mice and also in adult *Ivl*−/− mice up to 2 years of age in pathogen-free housing conditions (data not shown). An additional interpretation is that the presence of involucrin may promote a niche-specific microbiome with enrichment for specific members of the Firmicutes, Proteobacteria, and Bacteroidetes

phyla at the expense of the Bacteriodetes phylum, *Muribaculaceae*, and distinct members of the Firmicutes and Verrumocrobia phyla.

Until now, our current understanding of human skin evolution has been illuminated with the discovery of skin pigmentation as an adaptation to the degree of UVB sun exposure (Jablonski and Chaplin, 2010). Our current research expands our understanding of skin evolution with the identification of IVL-mediated adaptation for the epidermis. Our previous work identified recent positive selection for increased *IVL* in European populations (Mathyer et al., 2021) suggesting a functional role for *IVL* dosage that we addressed in this paper. Indeed, earlier studies have highlighted genetic innovation for *IVL* with the expansion of glutamine-rich tandem repeats across mammalian and primate clades and the more recent emergence of the “late” repeat domain that arose only in humans and continues to expand in repeat number across human populations (Eckert and Green, 1986, Djian and Green, 1989, Teumer and Green, 1989, Tseng and Green, 1989). In conclusion, our findings highlight an exciting paradigm for involucrin dosage to modulate vitamin D receptor function that affects epidermal crosstalk and modulation of the skin immune system.

MATERIALS AND METHODS

Mice

WT and *Ivl* −/− C57BL/6 mice were group-housed in pathogen-free, barrier conditions and approved by the Division of Comparative Medicine Animal Studies Committee (Washington University in St. Louis School of Medicine) and in accordance with the NIH Guide for the Care and Use of Laboratory Animals. MC903 treatment (1 nmol) was administered daily to the same ear (ethanol control on the opposite ear) in 11–14 week-old mice for 12 days. Ear thickness was measured daily with a Peacock dial thickness gauge caliper (Ozaki MFG, Japan).WT and *Ivl* −/− C57BL/6 mice were group-housed in pathogen-free, barrier conditions and approved by the Division of Comparative Medicine Animal Studies Committee (Washington University in St. Louis School of Medicine) and in accordance with the NIH Guide for the Care and Use of Laboratory Animals. MC903 treatment (1 nmol) was administered daily to the same ear (ethanol control on the opposite ear) in 11–14 week-old mice for 12 days. Ear thickness was measured daily with a Peacock dial thickness gauge caliper (Ozaki MFG, Japan).

Flow Cytometry

MC903-treated ear tissue was dissociated (0.25% Trypsin/EDTA) at 37 °C (750 rpm) for 90 mins and Fc receptor was blocked. Antibodies are listed in Supplementary Material. Gates were based on the specificity of cell surface marker vs. isotype control staining with dead cell exclusions (Hoechst or 7AAD positive) via BD FACSAria II and FlowJo10.6.2 analysis.

scRNA-seq

Treated ears were dissociated in trypsin at 37°C (750 rpm) for 90 minutes and strained prior to two rounds of centrifugation (300 rcf) for 7 mins at 4°C. A total of 20,000 live cells (Hoechst$^-$) per sample were captured by flow cytometry (AriaII) and submitted for 10X Genomics library preparation and sequencing. Unfiltered feature-barcode matrix per sample

from 10X Cell Ranger was obtained for each *Ivl* −/− and WT replicate (n=2 per genotype). Analysis was performed with the R programming environment (v4.1.0) and Seurat (v4.0.3) (Hao et al., 2021). Cells were excluded for any of the following criteria: cell of low quality (< 700 genes), cell "doublets" (>8000 genes), and dead/stressed cell (> 60% mitochondrial gene expression). *Ivl* −/− single cells were down-sampled to the WT populations (8135 cells per genotype). All data was scaled and normalized with the centered-log ratios parameter, followed by principal component analysis (10 principal components), and batch correction and integration using Harmony (Korsunsky et al., 2019). UMAP was determined by FindNeighbors using dimensions 1 through 10 as input parameter and FindClusters with a resolution of 0.8 for cell cluster discovery using the Louvain algorithm. Marker genes were identified separately for each genotyped samples using FindAllMarkers function. Cell clusters were determined by comparing reference datasets in (Joost et al., 2016) and My Geneset on Immunological Genome Project (immgen.org). Analysis of vitamin D responsive genes involved the comparisons of gene expression means for genes listed in GSEA Mouse Gene Set: GOBP_CELLULAR_RESPONSE_TO_VITAMIN_D (MM9698) (Subramanian et al., 2005) (Liberzon et al., 2015).

Microbiome

Skin microbiota was collected using pre-moistened sterile swabs on adult mouse ear skin (co-housed littermates by genotype) prior to and after 12 days of MC903 treatment (n=3, WT and *Ivl* −/− each). Air swabs from each cage were obtained as negative controls. Bacterial swabs were subject to bacterial genome isolation and submitted for 16S rRNA microbiome sequencing (V1-V3 regions) on Illumina Miseq. A total of ~720,000 reads were obtained with mean of 30k and median of 29k per sample. Quality control was performed with AlignerBoost v1.8.3 (Zheng and Grice, 2016) and demultiplexed with Flexbarv3.5 (Roehr et al., 2017). Chloroplast and mitochondrial reads that mapped to the taxonomy class Chloroplast or family mitochondria were removed from the analysis. Phylogenetic assignment was obtained using HmmUFOtuv1.4.2 (Zheng et al., 2018)with the GreenGene97% OTU database (release 13.8) database and pseudo-node on (all OTUs as leaf nodes). Statistics were calculated using R package phyloseq v1.32.0 (McMurdie and Holmes, 2013)and DEseq2v1.28.1 (Love et al., 2014). To identify differentially enriched OTUs (DE-OTUs), 16s microbiome data were converted to DESeq2 objects and ran using a negative binomial linear model as ~ study_group*time_point. Thresholds for significant DE-OTUs were FDR < 0.1 and absolute $\log_2$FC >= 1.

Supplementary Material

Refer to Web version on PubMed Central for supplementary material.

ACKNOWLEDGEMENTS

We thank Fiona Watt for the Ivl-/- mice; Lloyd Miller for helpful discussion, Pascaline Akitani, Dorjan Brinja, and Erica Lantelme at the Flow Cytometry and Fluorescence Activated Cell Sorting Core, Jennifer Ponce and Mirhanda Allen at the Genome Technology Access Core (GTAC) at the McDonnell Genome Institute for scRNA-seq library prep, sequencing, and preliminary analyses, Jordan Harris in the Grice lab for DNA extraction, Simon Knight in the Grice lab for microbiota genomic isolation, Penn CHOP Microbiome Core for library prep and sequencing, and John Edwards for bioinformatics assistance. Support for this work was provided by the Society of Investigative Dermatology Sun Pharma Post-doctoral Award (M.E.M.), NIH/NHGRI T32 HG000045 (A.D.S.),

NIH/NHGRI R25HG006687 (Opportunities in Genomics Research training, C.M.), NIH/NCRR/NCI P30CA91842 (GTAC), NIH/NIAMS P30AR69589 (Penn Skin Biology and Diseases Resource-based Center), and NIH/NIAMS R01AR065523, R56AR075427, and R01AR079888 (C.dG.S.) funds. The content is solely the responsibility of the authors and does not necessarily represent the official views of the National Institutes of Health.

CONFLICT OF INTEREST STATEMENT

C.dG.S. and Erin A. Brettmann are listed as inventors on utility patent application 63/090,801 submitted by Washington University in St. Louis for the compositions and methods of involucrin for treating skin diseases, disorders, or conditions. C.dG.S. is the founder of Evoly Skin, LLC that is developing new technologies for skin barrier health.

DATA AVAILABILITY STATEMENT

Datasets related to this article can be found at https://www.ncbi.nlm.nih.gov/bioproject/PRJNA821259/, hosted at NCBI SRA, BioProject accession PRJNA821259 and at https://www.ncbi.nlm.nih.gov/bioproject/PRJNA786852/, hosted at NCBI SRA, BioProject accession PRJNA786852.

Abbreviations

AF	allele frequency
CE	cornified envelope
DE-OTU	differentially enriched operational taxonomic unit
EDC	Epidermal Differentiation Complex
Envl	envoplakin
eQTL	expression quantitative trait loci
IVL	involucrin
OTU	operational taxonomic unit
Ppl	periplakin
scRNA-seq	single-cell RNA sequencing
UMAP	uniform manifold approximation and projection
VDR	vitamin D receptor
WT	wild-type

REFERENCES

Bikle D, Christakos S. New aspects of vitamin D metabolism and action - addressing the skin as source and target. Nat Rev Endocrinol 2020;16(4):234–52. [PubMed: 32029884]

Bikle DD. Vitamin D metabolism and function in the skin. Mol Cell Endocrinol 2011;347(1–2):80–9. [PubMed: 21664236]

Bikle DD, Elalieh H, Chang S, Xie Z, Sundberg JP. Development and progression of alopecia in the vitamin D receptor null mouse. J Cell Physiol 2006;207(2):340–53. [PubMed: 16419036]

Carlberg C Molecular basis of the selective activity of vitamin D analogues. J Cell Biochem 2003;88(2):274–81. [PubMed: 12520526]

Chen J, Doroudi M, Cheung J, Grozier AL, Schwartz Z, Boyan BD. Plasma membrane Pdia3 and VDR interact to elicit rapid responses to 1alpha,25(OH)(2)D(3). Cell Signal 2013;25(12):2362–73. [PubMed: 23896121]

de Guzman Strong C, Conlan S, Deming CB, Cheng J, Sears KE, Segre JA A milieu of regulatory elements in the epidermal differentiation complex syntenic block: implications for atopic dermatitis and psoriasis. Hum Mol Genet 2010;19(8):1453–60. [PubMed: 20089530]

DeSantis TZ, Hugenholtz P, Larsen N, Rojas M, Brodie EL, Keller K, et al. Greengenes, a chimera-checked 16S rRNA gene database and workbench compatible with ARB. Appl Environ Microbiol 2006;72(7):5069–72. [PubMed: 16820507]

Djian P, Easley K, Green H. Targeted ablation of the murine involucrin gene. J Cell Biol 2000;151(2):381–8. [PubMed: 11038184]

Djian P, Green H. Vectorial expansion of the involucrin gene and the relatedness of the hominoids. Proc Natl Acad Sci U S A 1989;86(21):8447–51. [PubMed: 2813403]

Eckert RL, Green H. Structure and evolution of the human involucrin gene. Cell 1986;46(4):583–9. [PubMed: 2873896]

Hahn JM, Supp DM. Abnormal expression of the vitamin D receptor in keloid scars. Burns 2017;43(7):1506–15. [PubMed: 28778755]

Hao Y, Hao S, Andersen-Nissen E, Mauck WM 3rd, Zheng S, Butler A, et al. Integrated analysis of multimodal single-cell data. Cell 2021;184(13):3573–87 e29.

Horiuchi N, Clemens TL, Schiller AL, Holick MF. Detection and developmental changes of the 1,25-(OH)2-D3 receptor concentration in mouse skin and intestine. J Invest Dermatol 1985;84(6):461–4. [PubMed: 2987364]

Hosomi J, Hosoi J, Abe E, Suda T, Kuroki T. Regulation of terminal differentiation of cultured mouse epidermal cells by 1 alpha,25-dihydroxyvitamin D3. Endocrinology 1983;113(6):1950–7. [PubMed: 6196178]

Hussain M, Borcard L, Walsh KP, Pena Rodriguez M, Mueller C, Kim BS, et al. . Basophil-derived IL-4 promotes epicutaneous antigen sensitization concomitant with the development of food allergy. J Allergy Clin Immunol 2018;141(1):223–34 e5.

Igawa S, Di Nardo A. Skin microbiome and mast cells. Transl Res 2017;184:68–76. [PubMed: 28390799]

Jablonski NG, Chaplin G. Colloquium paper: human skin pigmentation as an adaptation to UV radiation. Proc Natl Acad Sci U S A 2010;107 Suppl 2:8962–8. [PubMed: 20445093]

Joost S, Zeisel A, Jacob T, Sun X, La Manno G, Lonnerberg P, et al. Single-Cell Transcriptomics Reveals that Differentiation and Spatial Signatures Shape Epidermal and Hair Follicle Heterogeneity. Cell Syst 2016;3(3):221–37 e9.

Kajava AV. alpha-Helical solenoid model for the human involucrin. FEBS Lett 2000;473(2):127–31. [PubMed: 10812058]

Kim BS, Siracusa MC, Saenz SA, Noti M, Monticelli LA, Sonnenberg GF, et al. TSLP elicits IL-33-independent innate lymphoid cell responses to promote skin inflammation. Sci Transl Med 2013;5(170):170ra16.

Kim BS, Wang K, Siracusa MC, Saenz SA, Brestoff JR, Monticelli LA, et al. Basophils promote innate lymphoid cell responses in inflamed skin. J Immunol 2014;193(7):3717–25. [PubMed: 25156365]

Kobayashi T, Glatz M, Horiuchi K, Kawasaki H, Akiyama H, Kaplan DH, et al. Dysbiosis and Staphylococcus aureus Colonization Drives Inflammation in Atopic Dermatitis. Immunity 2015;42(4):756–66. [PubMed: 25902485]

Korsunsky I, Millard N, Fan J, Slowikowski K, Zhang F, Wei K, et al. Fast, sensitive and accurate integration of single-cell data with Harmony. Nat Methods 2019;16(12):1289–96. [PubMed: 31740819]

Li M, Hener P, Zhang Z, Kato S, Metzger D, Chambon P Topical vitamin D3 and low-calcemic analogs induce thymic stromal lymphopoietin in mouse keratinocytes and trigger an atopic dermatitis. Proc Natl Acad Sci U S A 2006;103(31):11736–41.

Liberzon A, Birger C, Thorvaldsdottir H, Ghandi M, Mesirov JP, Tamayo P. The Molecular Signatures Database (MSigDB) hallmark gene set collection. Cell Syst 2015;1(6):417–25. [PubMed: 26771021]

Love MI, Huber W, Anders S. Moderated estimation of fold change and dispersion for RNA-seq data with DESeq2. Genome Biol 2014;15(12):550. [PubMed: 25516281]

Makin G, Lohnes D, Byford V, Ray R, Jones G. Target cell metabolism of 1,25-dihydroxyvitamin D3 to calcitroic acid. Evidence for a pathway in kidney and bone involving 24-oxidation. Biochem J 1989;262(1):173–80. [PubMed: 2818561]

Mathyer ME, Brettmann EA, Schmidt AD, Goodwin ZA, Oh IY, Quiggle AM, et al. Selective sweep for an enhancer involucrin allele identifies skin barrier adaptation out of Africa. Nat Commun 2021;12(1):2557. [PubMed: 33963188]

Matsui T, Amagai M. Dissecting the formation, structure and barrier function of the stratum corneum. Int Immunol 2015;27(6):269–80. [PubMed: 25813515]

McMurdie PJ, Holmes S. phyloseq: an R package for reproducible interactive analysis and graphics of microbiome census data. PLoS One 2013;8(4):e61217.

Meisel JS, Sfyroera G, Bartow-McKenney C, Gimblet C, Bugayev J, Horwinski J, et al. Commensal microbiota modulate gene expression in the skin. Microbiome 2018;6(1):20. [PubMed: 29378633]

Mischke D, Korge BP, Marenholz I, Volz A, Ziegler A. Genes encoding structural proteins of epidermal cornification and S100 calcium-binding proteins form a gene complex ("epidermal differentiation complex") on human chromosome 1q21. J Invest Dermatol 1996;106(5):989–92. [PubMed: 8618063]

Moosbrugger-Martinz V, Schmuth M, Dubrac S. A Mouse Model for Atopic Dermatitis Using Topical Application of Vitamin D3 or of Its Analog MC903. Methods Mol Biol 2017;1559:91–106. [PubMed: 28063040]

Moskovicz V, Ben-El R, Horev G, Mizrahi B. Skin microbiota dynamics following B. subtilis formulation challenge: an in vivo study in mice. BMC Microbiol 2021;21(1):231. [PubMed: 34418955]

Muehleisen B, Bikle DD, Aguilera C, Burton DW, Sen GL, Deftos LJ, et al. . PTH/PTHrP and vitamin D control antimicrobial peptide expression and susceptibility to bacterial skin infection. Sci Transl Med 2012;4(135):135ra66.

Nemes Z, Marekov LN, Steinert PM. Involucrin cross-linking by transglutaminase 1. Binding to membranes directs residue specificity. J Biol Chem 1999;274(16):11013–21.

Niec RE, Rudensky AY, Fuchs E. Inflammatory adaptation in barrier tissues. Cell 2021;184(13):3361–75. [PubMed: 34171319]

Oda Y, Uchida Y, Moradian S, Crumrine D, Elias PM, Bikle DD. Vitamin D receptor and coactivators SRC2 and 3 regulate epidermis-specific sphingolipid production and permeability barrier formation. J Invest Dermatol 2009;129(6):1367–78. [PubMed: 19052561]

Ormerod KL, Wood DL, Lachner N, Gellatly SL, Daly JN, Parsons JD, et al. Genomic characterization of the uncultured Bacteroidales family S24–7 inhabiting the guts of homeothermic animals. Microbiome 2016;4(1):36. [PubMed: 27388460]

Pillai S, Bikle DD, Elias PM. 1,25-Dihydroxyvitamin D production and receptor binding in human keratinocytes varies with differentiation. J Biol Chem 1988;263(11):5390–5. [PubMed: 2451669]

Quack M, Carlberg C. The impact of functional vitamin D(3) receptor conformations on DNA-dependent vitamin D(3) signaling. Mol Pharmacol 2000;57(2):375–84. [PubMed: 10648648]

Reddy GS, Tserng KY. Calcitroic acid, end product of renal metabolism of 1,25-dihydroxyvitamin D3 through C-24 oxidation pathway. Biochemistry 1989;28(4):1763–9. [PubMed: 2719932]

Ren D, Gong S, Shu J, Zhu J, Rong F, Zhang Z, et al. Mixed Lactobacillus plantarum Strains Inhibit Staphylococcus aureus Induced Inflammation and Ameliorate Intestinal Microflora in Mice. Biomed Res Int 2017;2017:7476467.

Rice RH, Green H. Presence in human epidermal cells of a soluble protein precursor of the cross-linked envelope: activation of the cross-linking by calcium ions. Cell 1979;18(3):681–94. [PubMed: 42494]

Robinson NA, LaCelle PT, Eckert RL Involucrin is a covalently crosslinked constituent of highly purified epidermal corneocytes: evidence for a common pattern of involucrin crosslinking in vivo and in vitro. J Invest Dermatol 1996;107(1):101–7. [PubMed: 8752847]

Roehr JT, Dieterich C, Reinert K. Flexbar 3.0 - SIMD and multicore parallelization. Bioinformatics 2017;33(18):2941–2. [PubMed: 28541403]

Romney ALT, Davis EM, Corona MM, Wagner JT, Podrabsky JE. Temperature-dependent vitamin D signaling regulates developmental trajectory associated with diapause in an annual killifish. Proc Natl Acad Sci U S A 2018;115(50):12763–8.

Sanin DE, Ge Y, Marinkovic E, Kabat AM, Castoldi A, Caputa G, et al. A common framework of monocyte-derived macrophage activation. Sci Immunol 2022;7(70):eabl7482.

Schauber J, Dorschner RA, Coda AB, Buchau AS, Liu PT, Kiken D, et al. Injury enhances TLR2 function and antimicrobial peptide expression through a vitamin D-dependent mechanism. J Clin Invest 2007;117(3):803–11. [PubMed: 17290304]

Schlingmann KP, Kaufmann M, Weber S, Irwin A, Goos C, John U, et al. Mutations in CYP24A1 and idiopathic infantile hypercalcemia. N Engl J Med 2011;365(5):410–21. [PubMed: 21675912]

Sevilla LM, Nachat R, Groot KR, Klement JF, Uitto J, Djian P, et al. Mice deficient in involucrin, envoplakin, and periplakin have a defective epidermal barrier. J Cell Biol 2007;179(7):1599–612. [PubMed: 18166659]

Steinert PM, Marekov LN The proteins elafin, filaggrin, keratin intermediate filaments, loricrin, and small proline-rich proteins 1 and 2 are isodipeptide cross-linked components of the human epidermal cornified cell envelope. J Biol Chem 1995;270(30):17702–11.

Stumpf WE, Sar M, Reid FA, Tanaka Y, DeLuca HF. Target cells for 1,25-dihydroxyvitamin D3 in intestinal tract, stomach, kidney, skin, pituitary, and parathyroid. Science 1979;206(4423):1188–90. [PubMed: 505004]

Subramanian A, Tamayo P, Mootha VK, Mukherjee S, Ebert BL, Gillette MA, et al. Gene set enrichment analysis: a knowledge-based approach for interpreting genome-wide expression profiles. Proc Natl Acad Sci U S A 2005;102(43):15545–50.

Teumer J, Green H. Divergent evolution of part of the involucrin gene in the hominoids: unique intragenic duplications in the gorilla and human. Proc Natl Acad Sci U S A 1989;86(4):1283–6. [PubMed: 2919176]

Tseng H, Green H. The involucrin gene of the owl monkey: origin of the early region. Mol Biol Evol 1989;6(5):460–8. [PubMed: 2507864]

Uberoi A, Bartow-McKenney C, Zheng Q, Flowers L, Campbell A, Knight SAB, et al. Commensal microbiota regulates skin barrier function and repair via signaling through the aryl hydrocarbon receptor. Cell Host Microbe 2021;29(8):1235–48 e8.

Villani AC, Satija R, Reynolds G, Sarkizova S, Shekhar K, Fletcher J, et al. . Single-cell RNA-seq reveals new types of human blood dendritic cells, monocytes, and progenitors. Science 2017;356(6335).

Volz A, Korge BP, Compton JG, Ziegler A, Steinert PM, Mischke D. Physical mapping of a functional cluster of epidermal differentiation genes on chromosome 1q21. Genomics 1993;18(1):92–9. [PubMed: 8276421]

Walsh CM, Hill RZ, Schwendinger-Schreck J, Deguine J, Brock EC, Kucirek N, et al. Neutrophils promote CXCR3-dependent itch in the development of atopic dermatitis. Elife 2019;8.

Wang Z, Mascarenhas N, Eckmann L, Miyamoto Y, Sun X, Kawakami T, et al. Skin microbiome promotes mast cell maturation by triggering stem cell factor production in keratinocytes. J Allergy Clin Immunol 2017;139(4):1205–16 e6.

Watt FM. Mammalian skin cell biology: at the interface between laboratory and clinic. Science 2014;346(6212):937–40. [PubMed: 25414300]

Xie Z, Komuves L, Yu QC, Elalieh H, Ng DC, Leary C, et al. Lack of the vitamin D receptor is associated with reduced epidermal differentiation and hair follicle growth. J Invest Dermatol 2002;118(1):11–6. [PubMed: 11851870]

Zhang C, Dowd DR, Staal A, Gu C, Lian JB, van Wijnen AJ, et al. Nuclear coactivator-62 kDa/Ski-interacting protein is a nuclear matrix-associated coactivator that may couple vitamin D receptor-mediated transcription and RNA splicing. J Biol Chem 2003;278(37):35325–36.

Zhao XP, Elder JT. Positional cloning of novel skin-specific genes from the human epidermal differentiation complex. Genomics 1997;45(2):250–8. [PubMed: 9344646]

Zheng Q, Bartow-McKenney C, Meisel JS, Grice EA HmmUFOtu: An HMM and phylogenetic placement based ultra-fast taxonomic assignment and OTU picking tool for microbiome amplicon sequencing studies. Genome Biol 2018;19(1):82. [PubMed: 29950165]

Zheng Q, Grice EA. AlignerBoost: A Generalized Software Toolkit for Boosting Next-Gen Sequencing Mapping Accuracy Using a Bayesian-Based Mapping Quality Framework. PLoS Comput Biol 2016;12(10):e1005096.

Zilionis R, Engblom C, Pfirschke C, Savova V, Zemmour D, Saatcioglu HD, et al. Single-Cell Transcriptomics of Human and Mouse Lung Cancers Reveals Conserved Myeloid Populations across Individuals and Species. Immunity 2019;50(5):1317–34 e10.

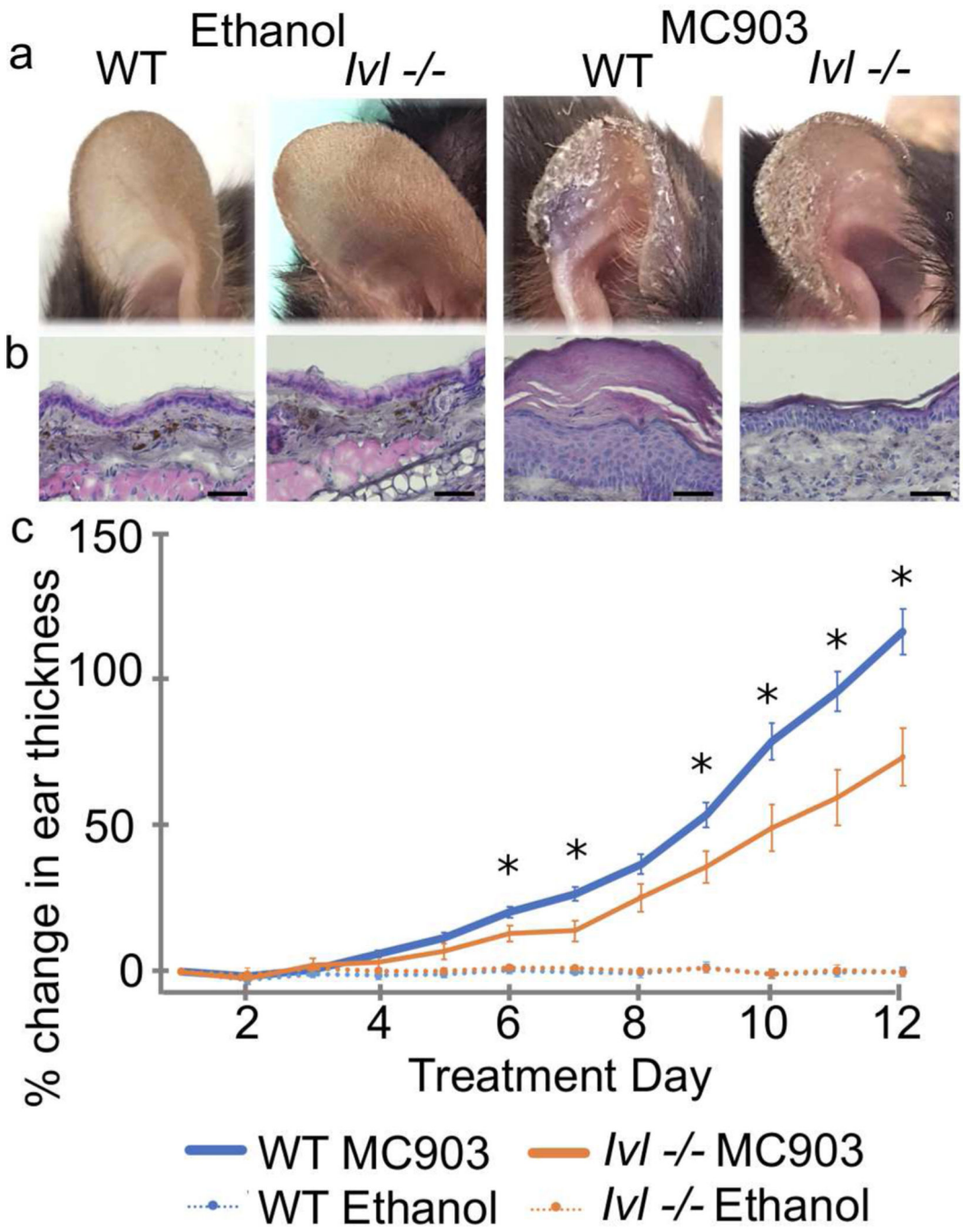

Figure 1. Reduced Vdr-mediated inflammation in MC903-treated *Ivl* −/− mouse skin.

(a) MC903-treated *Ivl* −/− mouse ears displayed less scaling and thickness compared to WT. **(b)** Hematoxylin and eosin histology staining revealed epidermal hyperkeratosis and hyperplasia in WT ear skin vs. *Ivl* −/−. Scale bar = 50 μm. **(c)** Percent change in ear thickness (inflammation) was significantly reduced in MC903-treated *Ivl* −/− (n=10, orange) vs. WT mice (n=15, blue) at days 6 and 7 and days 9–12 vs. day 0. *$p < 0.05$, one-way ANOVA with post-hoc Tukey HSD. Error bars ±SEM. No percent change was observed in ethanol-treated control ears (*Ivl* −/−, n=10, dotted orange; WT, n=15, dotted blue). Vdr,

vitamin D receptor; Ivl, Involucrin; WT, wild-type; ANOVA, ANalysis Of VAriance; HSD, Honestly Significant Difference.

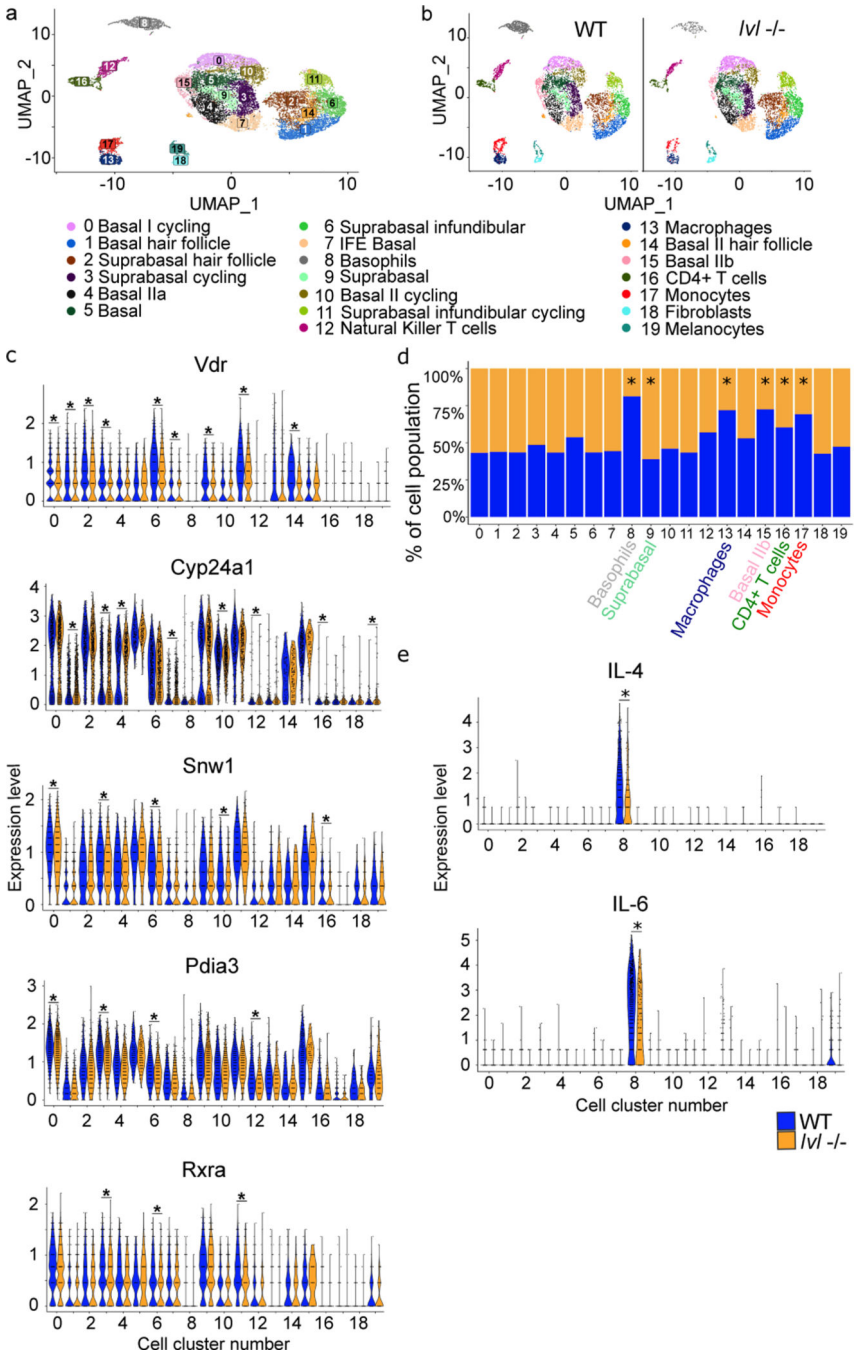

Figure 2. scRNA-seq identifies differential expressions for Vitamin D-responsive genes and decreases in basophils, macrophages, CD4+ T cells, monocytes, and basal II keratinocytes and an increase in suprabasal keratinocytes in MC903-treated *Ivl* −/− skin.

(a) UMAP of scRNA-seq-identified cell types in both MC903-treated WT and *Ivl* −/− skin (n=2/genotype). **(b)** Individual UMAPs of cell types in MC903-treated WT (left) and *Ivl* −/− (right) skin. **(c)** Vitamin D-responsive *Vdr*, *Cyp24a1*, *Snw1*, *Pdia3*, and *Rxra* genes are differentially expressed between MC903-treated WT and *Ivl* −/− skin and ranked by number of clusters with significance and by number found in keratinocyte clusters (Wilcoxon signed-rank test, *adj. p <0.05, see also Table S3). **(d)** Bar plots (proportions of cells)

for *Ivl* −/− (orange) and WT (blue). Basophils, macrophages, CD4+ T cells, monocytes, and basal II keratinocytes were decreased. Suprabasal keratinocytes were increased in *Ivl* −/− vs. WT (chi-squared goodness of fit, $*p < 0.05$). **(e)** Predominant IL-4 and IL-6 expressions in basophils that were reduced in MC903-treated *Ivl*−/− vs. WT skin. Ivl, Involucrin; WT, wild-type; UMAP, Uniform Manifold Approximation and Projection.

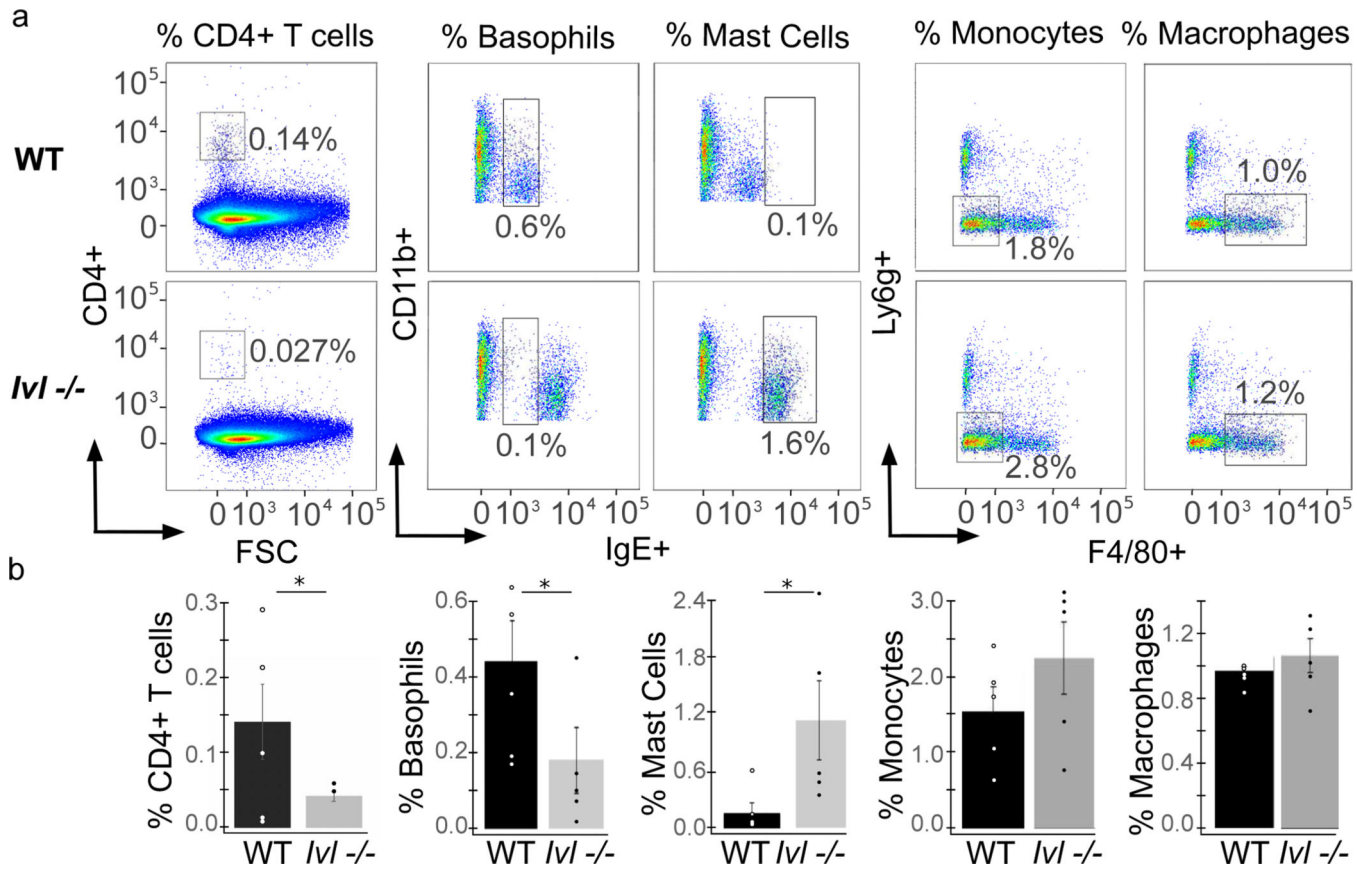

Figure 3. CD4$^+$ T cells and CD11b$^+$ IgE$^+$ basophils are reduced and CD11b$^+$ IgE^{high} mast cells are increased in MC903-treated *Ivl* −/− mouse skin.

(a) Flow cytometry pseudocolor dot plots for CD45$^+$ gated cell types shown in representative MC903-treated WT and *Ivl* −/− ear skin (day 12). **(b)** Bar graphs of cell type mean percentages are also shown. CD4$^+$ T cells and CD11b$^+$ IgE$^+$ basophils in MC903-treated *Ivl* −/− ear skin were significantly decreased. CD11b$^+$ IgE^{high} mast cells were also significantly increased in MC903-treated *Ivl* −/− ear skin. (CD4$^+$ T cells, $*p < 0.04$; basophils, $p < 0.05$; mast cells, $*p < 0.03$, one-sided *t*-test). No significant differences were found for both monocytes and macrophages (n=5/genotype). Error bars ±SEM. Ivl, Involucrin; WT, wild type.

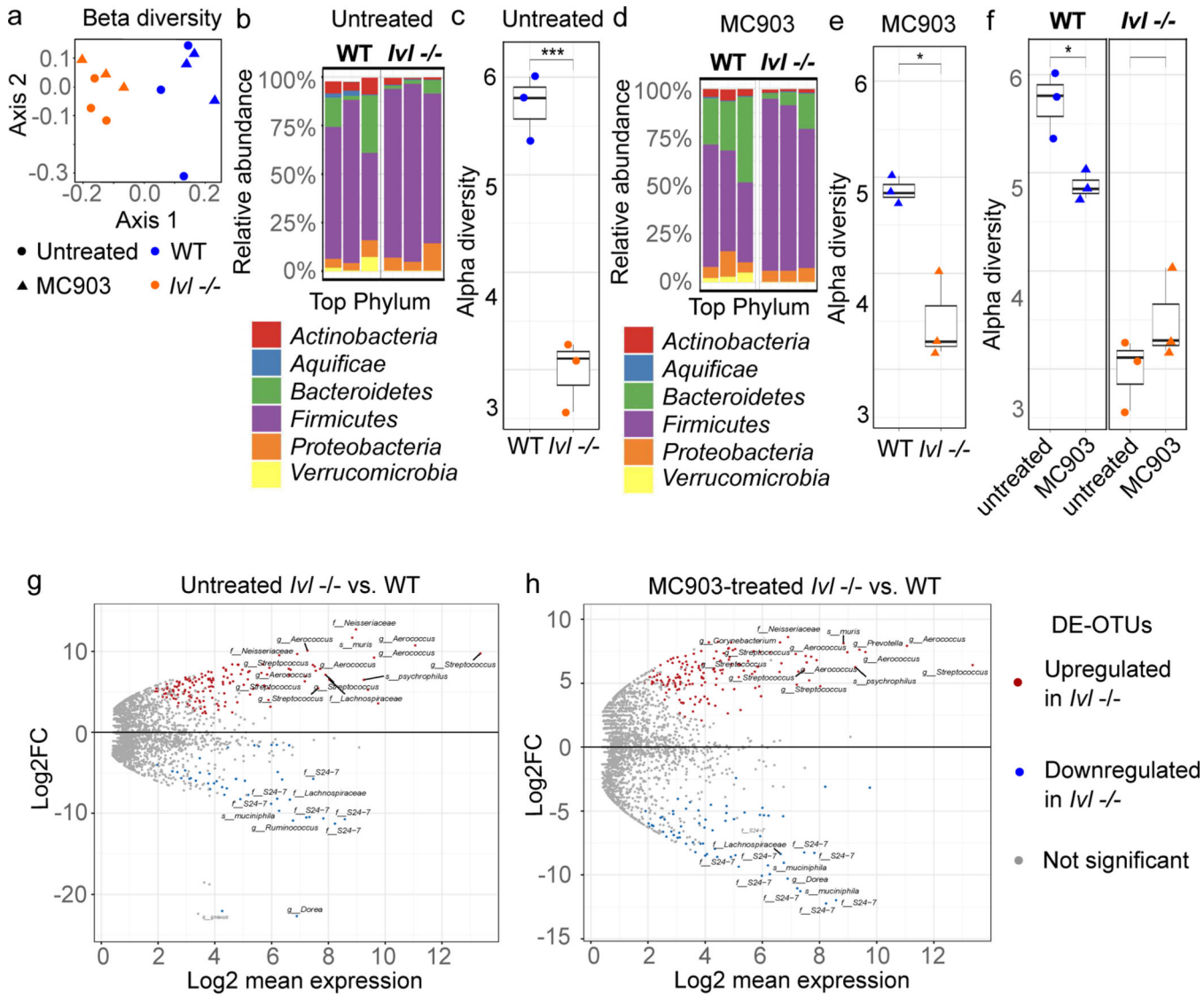

Figure 4. MC903-treated WT skin show increased Bacteroidetes and decreased Firmicutes whereas *Ivl* −/− untreated skin exhibit increased *Streptococcus* and *Aerococcus* (Firmicutes) and decreased *Muribaculaceae* (Bacteroidetes) taxa.

(a) Clustering between microbial communities based on unweighted UniFrac distance (beta diversity) was significantly associated with both genotype (WT or *Ivl* −/−) and MC903 treatment (before or after). Axis 1 (26.1% variance) and Axis 2 (16.3% variance) (OTU_dist ~ study_group * TimePoint, $p < 0.005$). **(b)** Relative abundance of top phylum-level OTUs in untreated WT and *Ivl* −/− skin (WT and *Ivl* −/−, each n=3). **(c)** Decreased alpha diversity (Shannon index) in untreated *Ivl* −/− vs. WT skin (***$p < 0.01$). **(d)** Relative abundance of top phylum-level OTUs in MC903-treated WT and *Ivl* −/− skin. **(e)** Decreased alpha diversity in MC903-treated *Ivl* −/− vs. WT skin (*$p < 0.05$). **(f)** Alpha diversity is significantly reduced in MC903-treated WT skin (*$p < 0.05$) but not in MC903-treated *Ivl* −/− skin. DE-OTU MA plots of **(g)** untreated *Ivl* −/− vs. WT skin; *Streptococcus*, *Aerococcus*, *Lachnospiraceae,* and *Muris* (phylum Firmicutes) comprise a majority of top 15 significantly upregulated DE-OTUs and *Muribaculaceae* (phylum Bacteroidetes) represent

the most common top 15 significantly downregulated DE-OTUs and **(h)** MC903-treated *Ivl* −/− vs. WT skin; *Streptococcus* and *Aerococcus* are also found in a majority of top 15 significantly upregulated DE-OTUs with *Muribaculaceae* in a majority of the top 15 significantly downregulated DE-OTUs. All MA plots shown with FDR < 0.1, log2FC>=1. Ivl, Involucrin; WT, wild-type; DE-OTUs, differentially expressed operational taxonomic units; FDR, false discovery rate; log2FC, log-fold change.